

Linear TMC-95-Based Proteasome Inhibitors

Nicolas Basse,[‡] Sandrine Piguel,[†] David Papapostolou,[‡] Alexandra Ferrier-Berthelot,[†] Nicolas Richy,[†] Maurice Pagano,[‡] Pierre Sarthou,[#] Joëlle Sobczak-Thépot,[#] Michèle Reboud-Ravaux,^{*,‡} and Joëlle Vidal^{*,†}

Laboratoire d'Enzymologie Moléculaire et Fonctionnelle, FRE 2852, CNRS, Université de Paris VI, Institut Jacques Monod, T43, 2 Place Jussieu, F 75251 Paris Cedex 05, France, Laboratoire de Synthèse et Électrosynthèse Organiques, CNRS UMR 6510, Université de Rennes 1, Campus de Beaulieu, F 35042 Rennes Cedex, France, and Laboratoire de Biochimie Cellulaire, CNRS UMR 7098, Université Paris VI, 9 Quai Saint-Bernard, F-75252 Paris Cedex 05, France

Received February 2, 2007

We have designed and evaluated 45 linear analogues of the natural constrained cyclopeptide TMC-95A. These synthetically less demanding molecules are based on the tripeptide sequence Y-N-W of TMC-95A. Structural variations in the amino acid side chains and termini greatly influenced both the efficiency and selectivity of action on a given type of active site. Inhibition constants were submicromolar ($K_i \approx 300$ nM) despite the absence of the entropically favorable constrained conformation that is characteristic of TMC-95A and its cyclic analogues. These linear compounds were readily prepared and reasonably stable in culture medium and could be optimized to inhibit one, two, or all three proteasome catalytic sites. Cytotoxicity assays performed on a series of human tumor cell lines identified the most potent inhibitors in cells.

Introduction

The ubiquitin–proteasome pathway is central to intracellular protein homeostasis.¹ It is involved in processes like cell cycle regulation and cytokine-stimulated signal transduction.² The proteasome is a promising target for the treatment of diseases such as inflammation, immune diseases, and cancer.³ The FDA has approved the proteasome inhibitor bortezomib (Figure 1) for anticancer therapy.⁴ The eukaryotic 26S proteasome is composed of the catalytically competent 20S particle, which interacts with the regulatory 19S regulatory caps. The eukaryotic 20S proteasome is formed of four stacked α_1 – β_1 – β_1 – α_1 – β_1 multiprotein rings and has two copies of each of three distinct catalytic subunits. One is responsible for chymotrypsin-like activity (CT-L, attributed to β_5), the second for trypsin-like activity (T-L, β_2), and the third for post-glutamyl peptide hydrolysis or post-acid activity (PGPH or PA, β_1). Most proteasome inhibitors are short peptides bearing a reactive group such as aldehyde (MG132, calpain I inhibitor Ac-Leu-Leu-Nle-H, tyropeptin A, Figure 1), boronic acid (bortezomib, Figure 1), or vinyl sulfone that forms a covalent bond with the catalytic O^γ-Thr1 in the three catalytic sites.^{5,6} Some natural molecules (epoxomicin, lactacystin, homobelactosin, salinosporamide) and their synthetic derivatives (omuralide) also form covalent adducts.⁷

Noncovalent inhibitors have been investigated less extensively, although they should have weaker side effects in therapeutic applications. A few synthetic products (ritonavir,⁸ several benzylstatine derivatives⁹) and one natural product (TMC-95A,¹⁰ Figure 1) inhibit the proteasome noncovalently. TMC-95A is a constrained cyclic tripeptide containing original N- and C-terminal functions, a tyrosine–asparagine–highly oxidized tryptophan sequence, and a side chain bridge through a phenylhydroxyoxindole (biaryl) linkage. It inhibits all three

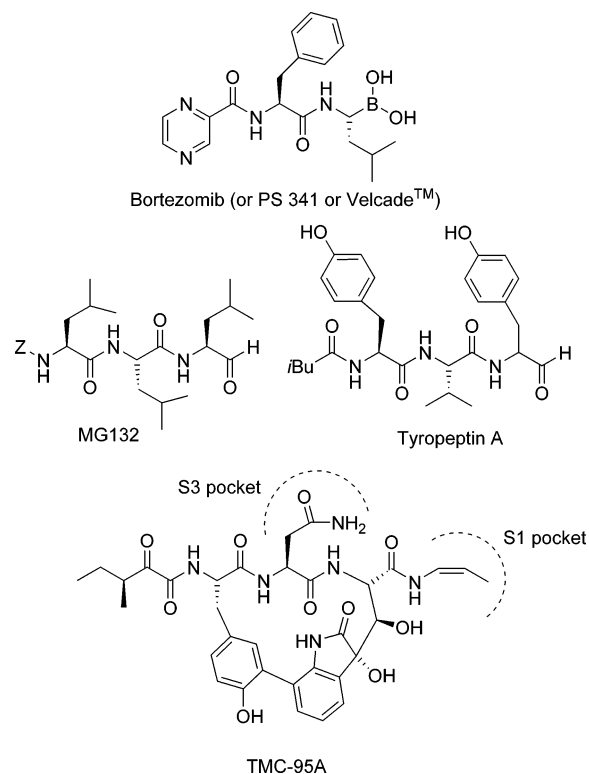


Figure 1. Some proteasome inhibitors. Binding of TMC-95A to proteasome S1 and S3 subsites is shown.¹²

proteasome activities (K_i of 0.0054 μ M for CT-L, 0.060 for PA, and 0.2 for T-L) and has antitumor activity.¹¹ Its binding to proteasome active sites has been characterized by X-ray crystallography.¹² The noncovalent interactions are mainly mediated by hydrogen bonds and lead to the formation of an antiparallel β sheet between the inhibitor and amino acid residues of the binding pockets with an additional hydrogen bond involving the oxygen of the oxindole group. The C-terminal (Z)-propenyl moiety acts as the P1 and the asparagine as the P3 residues. While the tyrosine residue interacts weakly with the hydrophobic S4 subsite, the hydroxyl groups of the oxidized tryptophan and the N-terminal 3-methyl-2-oxopen-

* To whom correspondence should be addressed. For M.R.-R.: phone, +33 1 44 27 50 78; fax, +33 1 44 27 59 94; e-mail, reboud@ccr.jussieu.fr. For J.V.: phone, +33 2 23 23 57 33; fax, +33 2 23 23 69 78; e-mail, joelle.vidal@univ-rennes1.fr.

[†] Université de Rennes 1.

[‡] Laboratoire d'Enzymologie Moléculaire et Fonctionnelle, Université de Paris 6.

[#] Laboratoire de Biochimie Cellulaire, Université de Paris 6.

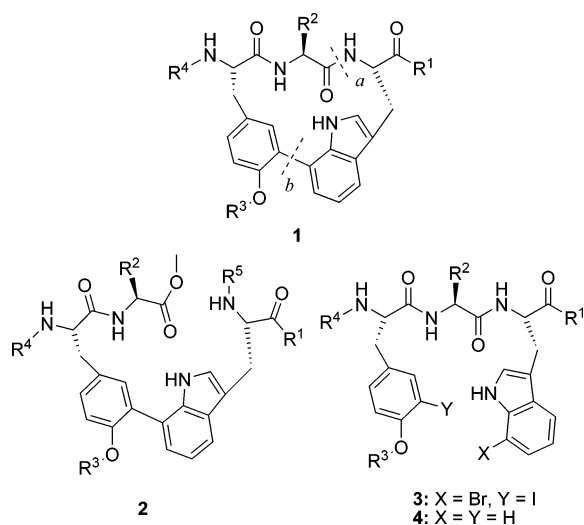
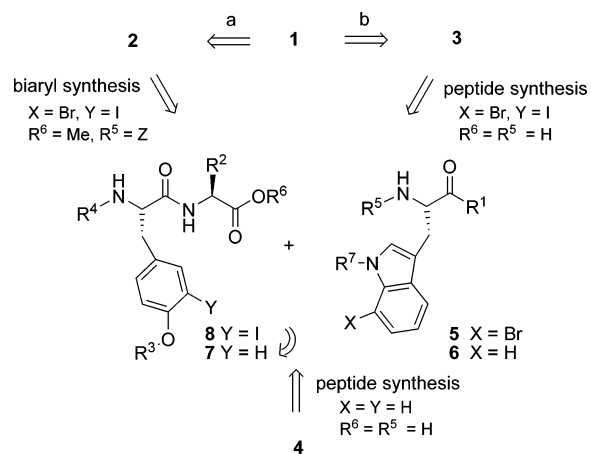


Figure 2. Structures of cyclic (**1**) and linear (**2–4**) compounds. The dotted lines *a* and *b* indicate the bonds chosen to be disrupted in order to generate (a) linear analogues **2** having a phenylindole group and (b) linear analogues **3** and **4** in which the tripeptide chain is retained.

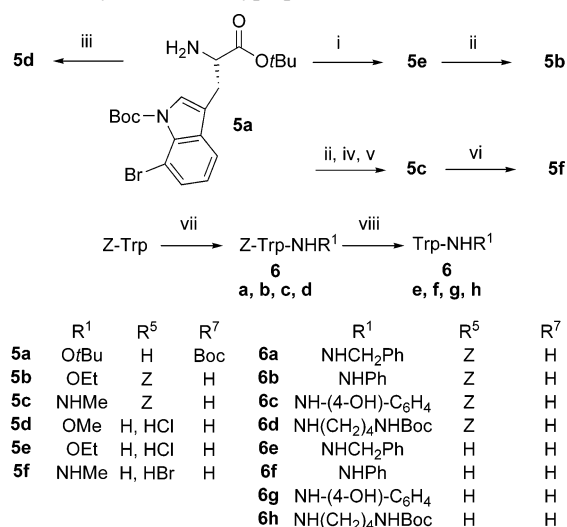
tanoyl group are exposed to the surface (Figure 1). The high-affinity binding of TMC-95A is mostly attributed to its constrained conformation mediated by the biaryl system. Total syntheses of this original 17-membered macrocycle have been achieved.^{13–15} Although some cyclic synthesis precursors had very interesting enzymatic properties, the complexity of their preparation still hinders their accessibility.¹⁶ Simpler cyclic rigid analogues of TMC-95A bearing a phenyloxindole linkage^{17,18} or a biphenyl ether linkage¹⁹ have also been described. Although their constrained conformation provides the driving force for entropically high-affinity binding, these derivatives are less strongly bound than TMC-95A.²⁰ We postulated that the structural elements of the natural product that are required for proteasome inhibition could be identified and used to design linear TMC-95A mimics that are less difficult to prepare than TMC-95A itself or its cyclic mimics. We have produced a library of linear mimics to selectively target one or more active sites.

We previously reported the synthesis of macrocycles **1** in which the peptide structure of TMC-95 was retained and the highly oxidized tryptophan was replaced by tryptophan (Figure 2).²¹ Their poor inhibition of rabbit 20S proteasome reported here prompted us to design the linear mimics of TMC-95A **2–4**. The oxidized tryptophan of TMC-95A was replaced by tryptophan in all these molecules; they also lacked the synthetically challenging hydroxy groups of tryptophan, 3-methyl-2-oxopentanoyl group at the N-terminus, and (*Z*)-prop-1-enyl moiety at the C-terminus (Figure 2). The objective was to determine how the catalytic activities of the 20S proteasome were influenced by elements derived from TMC-95A. Consequently, compounds **2** contain the phenylindole group but not the tripeptide sequence; compounds **3** and **4** contain the tripeptide sequence but not the phenylindole group. The tryptophan and tyrosine residues were kept in all cases, and the substituents R^1 , R^2 , R^3 , and R^4 and *X* and *Y* groups were varied. Compounds **3** contained nonproteogenic halogenated Trp and Tyr residues ($X = \text{Br}$, $Y = \text{I}$), while compounds **4** did not. This report describes the syntheses of three series of acyclic mimics of TMC-95A (compounds **2–4**), their activities and selectivities for 20S proteasome active sites, as well as that of cyclic mimics **1**, and their metabolic stability. The cytotoxic activities of the four most active inhibitors among the 45 newly synthesized compounds were assayed on several

Scheme 1. Convergent Retrosynthetic Pathway for Compounds **1–4**



Scheme 2. Syntheses of Tryptophan Derivatives **5** and **6**^a



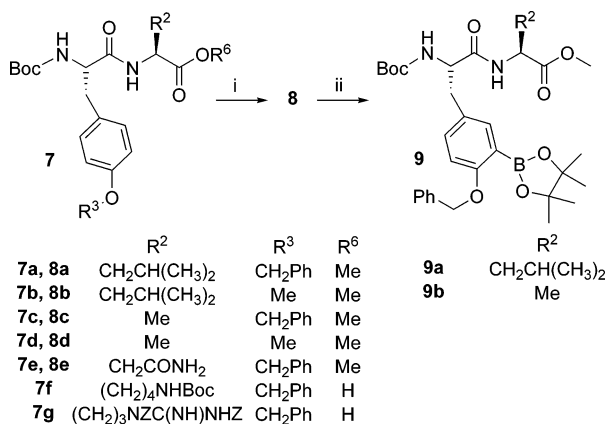
^a Reagents: (i) HCl, EtOH, 100%; (ii) ZOSu, DMF, 70% (for **5b**); (iii) HCl, MeOH, 100%; (iv) HCl, AcOEt; (v) ClCO₂Et, Et₃N, THF, then MeNH₂, THF, 81% from **5a**; (vi) HBr, AcOH, 100%; (vii) DCC, R^1 -NH₂, 31% (for **6a**), 69% (for **6b**), 77% (for **6c**), 82% (for **6d**); (viii) H₂, Pd/C, MeOH, DMF, 83% (for **6e**), 73% (for **6f**), 59% (for **6g**), 82% (for **6h**).

human tumor cell lines to evaluate their potentials as cytotoxic tumor agents.

Results and Discussion

Chemistry. A convergent retrosynthetic scheme was used to prepare compounds **1–4** (Scheme 1). Two major disconnections were evident for macrocycles **1**: the first (path *a*) led to biaryl compounds **2**, while the second (path *b*) led to tripeptides **3**.²¹ These synthons **2** and **3** required the same starting materials **5** and **8**, thereby making it possible to generate a library of analogues by varying R^1 , R^2 , R^3 , or R^4 . Tripeptides **4** were assembled in a similar convergent way from tryptophan derivatives **6** and dipeptides **7**, which were precursors of the iodized dipeptides **8**.

Derivative **5a** was the key compound for preparing unusual 7-bromotryptophans **5**, and gram quantities were synthesized as described previously,²¹ with a very high ee and in six steps from 1-bromo-2-nitrobenzene (Scheme 2). The functional groups of **5a** were transformed using general methods of peptide synthesis.²² The Boc protection in **5a** was removed with anhydrous HCl in alcohol (ethanol or methanol), and thus, transesterification led to amino esters **5d** or **5e** ($R^1 = \text{OEt}$ or

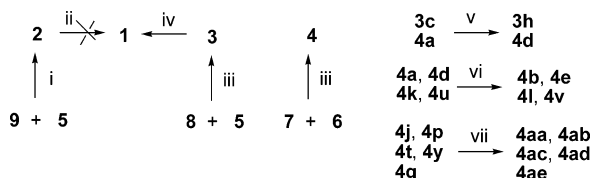
Scheme 3. Syntheses of Dipeptides **8** and **9**^a

^a Reagents and conditions: (i) I₂, Ag₂SO₄, EtOH, 72% (for **8a**), 85% (for **8b**), 85% (for **8c**), 72% (for **8d**), 69% (for **8e**); (ii) bis(pinacolato)diboron, PdCl₂dppf·CH₂Cl₂, KOAc, DMSO, 80 °C, 16 h, unseparated mixture of **9** and **7** (4.2/1 ratio for **9a/7a**, 7.8/1 ratio for **9b/7c**). See Supporting Information for the preparation of **7**.

OMe) as their hydrochloride salts. **5e** or **5a** was Z-protected using *N*-(benzyloxycarbonyloxy)succinimide. In the latter case, this protection was necessary for the introduction of the R¹ methylamide of **5c**. Acidolysis of the Boc and ^tBu group in AcOEt and coupling with methylamine by the mixed anhydride method led to the preparation of **5c** in 81% overall yield. The Z group in **5c** was removed to give **5f** under acid conditions (HBr/AcOH) because hydrogenation in the presence of palladium on charcoal also cleaved the carbon–bromine bond. The R¹ amide function in tryptophan derivatives **6a–d** was introduced by standard peptide coupling between Z-tryptophan and the corresponding amine in the presence of dicyclohexylcarbodiimide. Hydrogenolysis of the Z group in **6a–d** gave derivatives **6e–h** (Scheme 2).

Dipeptides **7** were prepared using conventional liquid-phase peptide synthesis²² from the succinimidyl active ester of Boc-tyrosine (Scheme 3). Dipeptides **7** were converted to iododipeptides **8** with I₂/Ag₂SO₄²³ in good yields. Standard Miyaura conditions²⁴ transformed **8a** and **8c** to a mixture of the corresponding pinacol boronates **9a** and **9b** along with **7a** and **7c** derived from a protodeboronation reaction.²⁵ Yields were estimated to be 57% for **9a** and 62% for **9b** by NMR, since **9** and **7** could not be separated by column chromatography (Scheme 3).

The last step in the syntheses was the combination of tryptophan building blocks **5** or **6** with dipeptide building blocks **7**, **8**, or **9** to generate a library of target compounds **1–4** (Scheme 4). Because of its mild reaction conditions, the Suzuki coupling²⁶ of forming aryl–aryl bonds²⁷ was used to build the biaryl linkage in **2** from boronate **9** and 7-bromotryptophan **5**. The reaction parameters (source of palladium, solvent, and base) were varied to identify optimal conditions,²⁸ and the desired biaryl products were obtained in yields of 94% (**2a**), 72% (**2b**), and 60% (**2c**) from 7-bromotryptophan derivatives **5b** or **5c**. The macrolactamization of properly deprotected biaryl products **2** was then investigated as a route to the macrocycles **1**. The methyl ester in **2** was saponified with LiOH in THF, and the Z protective group was cleaved along with the Bn group using H₂/Pd. The resulting crude mixture was subjected to various common peptide-coupling conditions (EDC/HOAT in CH₂Cl₂ or DMF, HATU in DMF, PyBOP/HOBt), but no cyclic product **1** was detected. Only trace amounts of the corresponding cyclic dimer were isolated (HRMS (ESI) measurement: calcd for

Scheme 4. Syntheses of Target Compounds **1–4**^a

^a See Table 1 for definitions of R¹, R², R³, and R⁴ groups in **1–4**. Reagents and conditions: (i) 20% mol Pd(OAc)₂, 10% mol P(*o*-tolyl)₃, Na₂CO₃/water, dioxane, 80 °C, 5 h, 94% (for **2a**), 72% (for **2b**), 60% (for **2c**); (ii) LiOH, THF, water, then H₂, Pd/C, MeOH, then EDC, HOAT, CH₂Cl₂ or HATU, DMF or PyBop, HOBt; (iii) **8a–e** or **7a–e**, LiOH, THF, water, then aqueous HCl, then EDC, HOBt, NEt₃, CH₂Cl₂, DMF, **5b–f** or **6e–h**, 81% (for **3a**), 71% (for **3b**), 70% (for **3c**), 88% (for **3d**), 47% (for **3e**), 67% (for **3f**), 54% (for **3g**), 43% (for **3i**), 56% (for **4a**), 63% (for **4f**), 45% (for **4g**), 48% (for **4h**), 66% (for **4i**), 67% (for **4j**), 49% (for **4k**), 31% (for **4m**), 30% (for **4n**), 75% (for **4o**), 63% (for **4p**), 42% (for **4q**), 44% (for **4r**), 78% (for **4s**), 68% (for **4t**), 20% (for **4u**), 31% (for **4w**), 28% (for **4x**), 33% (for **4y**), 65% (for **4z**); (iv) NiCl₂(PPh₃)₂, Zn, PPh₃, DMF, 4% (for **1a**), 8% (for **1b**), 10% (for **1c**); (v) LiOH, THF, water, then HCl, water, 82% (for **3h**), 80% (for **4c**), 64% (for **4d**); (vi) H₂, Pd/C, DMF, MeOH, 76% (for **4b**), 76% (for **4e**), 81% (for **4l**), 86% (for **4v**); (vii) anhydrous HCl/MeOH, 24% (for **4aa**), 38% (for **4ab**), 86% (for **4ac**), 26% (for **4ad**), 64% (for **4ae**).

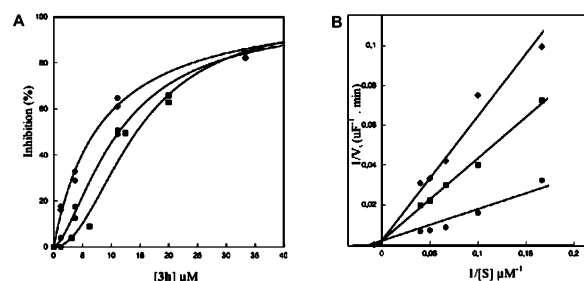


Figure 3. (A) Inhibition of CT-L (◆), PA (●), and T-L (■) activities of rabbit 20S proteasome by compound **3h**. The experimental data were fitted to equation % inhibition = 100[3h]/(IC₅₀ + [3h]) (◆) or % inhibition = 100[3h]^{n_H}/(IC₅₀^{n_H} + [3h]^{n_H}) with n_H = 1.5 (●) and 2 (■). (B) Double reciprocal Lineweaver–Burk plot for the inhibition of CT-L activity by **3h** with [3h] = 0 (●), 10 (■), 20 (◆) μM. Experimental points were fitted to the equation 1/V_i = (1 + [3h]/K_i)(K_m/V_m[S]) + 1/V_m.

[C₅₈H₇₀N₁₀O₁₂ + Na]⁺ 1121.5072, found 1121.5065). Similar results were reported by Kaiser et al.²⁹

Cyclization of the halogenated tripeptides **3** via formation of the aryl–aryl bond proved to be the most effective route to **1**, although yields were low (Scheme 4).²¹ Quantitative saponification of esters **8** followed by coupling with 7-bromotryptophan derivatives **5** in the presence of EDC/HOBt gave tripeptides **3** in moderate to good yields.²¹ Compounds **3a–c** were macrocyclized by Ni(0) mediated coupling of the aryl halides to form the biaryl linkage³⁰ of the corresponding constrained 17-membered macrocycles **1** in 4%, 8%, and 10% yields.²¹

Last, tripeptides **4** were readily obtained after saponification of dipeptides **7** and coupling with tryptophan derivatives **6** under low epimerizing conditions (EDC/HOBt). Tripeptides **3c** or **4** were deprotected under the usual conditions. Tripeptides **3c** or **4a** were saponified to give the corresponding acids **3h** or **4d**. The benzyl or Z groups were removed from **4a**, **4d**, **4k**, or **4u** by hydrogenolysis (H₂, Pd/C), and the Boc group in **4j**, **4p**, **4t**, **4y**, and **4g** was cleaved using anhydrous HCl.

Biology. The capacities of cyclic **1** and acyclic **2–4** analogues of TMC-95A to inhibit the three activities of rabbit 20S proteasome were assayed using appropriate fluorogenic substrates (Figure 3 and Table 1). The classical aldehyde proteasome inhibitor MG-132 (Z-Leu-Leu-Leu-H) (Figure 1) was used as standard. Cyclic analogues **1** that use the phenylindole as an

Table 1. Structures of Compounds 1–4 and Their Inhibition (or Activation) of Rabbit 20S Proteasome at pH 7.5 and 30 °C^a

compd	R ¹	R ²	R ³	R ⁴	K _i (μM) or activation factor <i>x</i>		
					CT-L	PA	T-L
1a	OMe	^t Bu	Bn	Boc	ni	>100	<i>x</i> = 1.4
1b	OMe	^t Bu	Me	Boc	ni	>100	<i>x</i> = 1.8
1c	OMe	Me	Me	Boc	ni	37.1	ni
2a	OE _t	^t Bu	Bn	Boc	ni	ni	<i>x</i> = 1.4
2b	NHMe	^t Bu	Bn	Boc	ni	ni	69
2c	NHMe	Me	Bn	Boc	ni	>100	21.5
3a	OMe	^t Bu	Bn	Boc	ni	ni	<i>x</i> = 2
3b	OMe	^t Bu	Me	Boc	ni	>100	<i>x</i> = 1.9
3c	OMe	Me	Bn	Boc	ni	96.4	ni
3d	OMe	Me	Me	Boc	59.3	74.0	ni
3e	OMe	CH ₂ CONH ₂	Bn	Boc	14.1	55.4	ni
3f	OE _t	^t Bu	Bn	Boc	ni	ni	ni
3g	OE _t	^t Bu	Me	Boc	ni	>100	ni
3h	OH	Me	Bn	Boc	1.6	2.8	3.0
3i	NHMe	Me	Bn	Boc	59.3	30.2	ni
4a	OMe	Me	Bn	Boc	44.8	>100	<i>x</i> = 9.8
4b	OMe	Me	H	Boc	9.2	8.7	<i>x</i> = 6
4c	OH	H	Bn	Boc	ni	ni	<i>x</i> = 1.8
4d	OH	Me	Bn	Boc	ni	ni	<i>x</i> = 1.5
4e	OH	Me	H	Boc	ni	ni	<i>x</i> = 6.8
4f	NHBn	H	Bn	Boc	ni	31.5	<i>x</i> = 1.7
4g	NHBn	Me	Bn	Boc	ni	55.4	<i>x</i> = 1.7
4h	NHBn	CH ₂ CONH ₂	Bn	Boc	59.3	84.2	<i>x</i> = 2.2
4i	NHBn	^t Bu	Bn	Boc	<i>x</i> = 1.3	ni	<i>x</i> = 1.9
4j	NHBn	(CH ₂) ₄ NHBoc	Bn	Boc	<i>x</i> = 1.3	ni	<i>x</i> = 1.8
4k	NHBn	(CH ₂) ₃ NZC(NH)NHZ	Bn	Boc	ni	ni	<i>x</i> = 1.9
4l	NHBn	(CH ₂) ₃ NHC(NH)NH ₂	H	Boc	1.2	0.6	3.9
4m	NHPh	Me	Bn	Boc	<i>x</i> = 1.4	ni	<i>x</i> = 1.6
4n	NHPh	CH ₂ CONH ₂	Bn	Boc	<i>x</i> = 1.5	ni	<i>x</i> = 2.5
4o	NHPh	^t Bu	Bn	Boc	ni	ni	<i>x</i> = 1.9
4p	NHPh	(CH ₂) ₄ NHBoc	Bn	Boc	ni	ni	<i>x</i> = 1.6
4q	NHC ₆ H ₄ OH	Me	Bn	Boc	65.7	1	ni
4r	NHC ₆ H ₄ OH	CH ₂ CONH ₂	Bn	Boc	>100	23.4	ni
4s	NHC ₆ H ₄ OH	^t Bu	Bn	Boc	ni	96.4	<i>x</i> = 1.6
4t	NHC ₆ H ₄ OH	(CH ₂) ₄ NHBoc	Bn	Boc	65.7	ni	>100
4u	NHC ₆ H ₄ OH	(CH ₂) ₃ NZC(NH)NHZ	Bn	Boc	ni	ni	ni
4v	NHC ₆ H ₄ OH	(CH ₂) ₃ NHC(NH)NH ₂	H	Boc	2.1	0.7	4.3
4w	NH(CH ₂) ₄ NHBoc	Me	Bn	Boc	<i>x</i> = 1.5	ni	<i>x</i> = 3.2
4x	NH(CH ₂) ₄ NHBoc	CH ₂ CONH ₂	Bn	Boc	<i>x</i> = 1.6	ni	<i>x</i> = 2.2
4y	NH(CH ₂) ₄ NHBoc	^t Bu	Bn	Boc	81.8	31.5	<i>x</i> = 2.3
4z	NH(CH ₂) ₄ NHBoc	(CH ₂) ₄ NHBoc	Bn	Boc	<i>x</i> = 1.6	ni	<i>x</i> = 1.9
4aa	NHBn	(CH ₂) ₄ NH ₂	Bn	H	1.07	ni	0.32
4ab	NHPh	(CH ₂) ₄ NH ₂	Bn	H	2.22	ni	1.12
4ac	NHC ₆ H ₄ OH	(CH ₂) ₄ NH ₂	Bn	H	0.85	ni	0.98
4ad	NH(CH ₂) ₄ NH ₂	^t Bu	Bn	H	3.69	22.5	0.33
4ae	NHBn	Me	Bn	H	0.48	>100	>100
MG132					0.075 ^b	0.67 ^b	4.5 ^b

^a ni: no inhibition at 100 μM. K_i > 100 μM: <20% inhibition at 100 μM. ^b IC₅₀ values obtained for MG132 under our experimental conditions.

endocyclic clamp were very poor inhibitors of PA activity and did not inhibit the CT-L and T-L activities. This confirms how difficult it is to obtain simplified cyclic TMC-95A analogues without any loss of inhibitory capacity.^{12b,16–19} Since the synthesis of the macrocycle is expensive and lengthy, we concentrated on acyclic compounds **2** and **3** in order to determine the influence of the phenylindole group (**2**) and the tripeptide moiety (**3**) on inhibition. Analogues **2**, which are generated by virtual disruption of the tripeptide chain of the cyclic compounds **1** (Figure 2), had no action on the CT-L and PA activities, but the amide derivatives **2b,c** (R¹ = NHMe) inhibited T-L activity. Because the peptide backbone of TMC-95A forms an antiparallel β sheet with residues of the S1 and S3 pockets of the active site clefts¹² (Figure 1), linear TMC-95A mimics that may fit into the individual clefts should be good inhibitors. We therefore synthesized the tripeptide compounds **3** and **4**. Several compounds **3** and **4** gave better inhibition of the three catalytic activities than did cyclic (**1**) and linear (**2**) compounds, depending on the structures of the R¹, R², R³, and R⁴ groups. In the yeast proteasome–TMC-95A complex, the side chain of asparagine is deeply inserted in the

S3 pocket. This lateral chain was replaced by the ^tBu group of leucine in compounds **3** (R² group) in order to increase specificity for the CT-L active site. Leucine is present in the calpain I inhibitor Ac-Leu-Leu-Ile-H. This substitution clearly abolished the inhibition of the three activities (**3e** versus **3a**, **3b**, **3f**, and **3g**), whereas the less bulky methyl was favorable (**3d**, **3h**, and **3i**; **3c** inhibits PA activity). This suggests that there must not be much bulk at this position if compounds **3** are to bind to the three catalytic sites. The nature of R³ (Me or Bn) had no apparent influence on inhibition, but changing the OMe (**3a**) R¹ group to NHMe (**3i**) showed the beneficial effect of the amide group. The competitive inhibitor **3h** was obtained by inserting the negatively charged carboxylate group at this position (R¹ = OH) (Figure 3); it had K_i values of 1.6 (CT-L), 2.8 (PA), and 3.0 (T-L) μM. The P1 residue (here, the R¹ substituent), together with potential P3 residue (here, the R² substituent), is an important modulator of the specific inhibition of CT-L, T-L, and PA activities. Compounds **4**, which have the same framework as compounds **3** with no halogen substitution on the indole and phenyl groups (Figure 2, X = Y = H), were studied because they are more readily prepared than **3**.

The negatively charged compounds **4c–e** ($R^1 = \text{OH}$) were not inhibitors (**4d** versus **3h**), whereas the amides ($R^1 = \text{NH-}$) were inhibitors (as in series **3**), as were the esters ($R^1 = \text{OMe}$) (unlike in series **3**). Aromatic amides ($R^1 = \text{NHBn}$ or $\text{NHC}_6\text{H}_4\text{OH}$) favored inhibition of PA activity alone (**4f–h**, **4r**, **4s**) when the R^2 groups were H, Me, or CONH_2 , but this effect was lost when the R^2 group was bulky (**4i–k,m–p,t,u**). But this result was modulated by the nature of the group R^1 since inhibition of PA activity was obtained with $R^1 = \text{NHC}_6\text{H}_4\text{OH}$ and $R^2 = i\text{Bu}$ (**4r**, **4s**). The NPh group prevented inhibition of all three proteasome activities (**4m–p**). A tyrosine at P1 favored inhibition by tyropeptin A aldehyde derivatives.³¹ The importance of an optimal fit into the S1 pocket of the three catalytic sites has been pointed out for endocyclic biphenyl ether compounds derived from TMC-95A, but binding to the S3 pocket is also essential.²⁰ The asparagine side chain at position R^2 , which may bind to the S3 subsite, favored the inhibition of CT-L activity because compounds containing H, Me, and $i\text{Bu}$ were not inhibitors (**4h** versus **4f**, **4g**, and **4i**). We then varied the T-L activity. Molecular modeling studies suggested that an R^2 group with chains of arginine or lysine would stimulate binding to the T-L active site. Thus, molecules bearing protected (**4k**, **4u**) or unprotected (**4l**, **4v**) arginine and protected (**4j**, **4p**, **4t**, **4z**) or unprotected (**4aa–c**) lysine lateral chains were evaluated. Molecules with protected lysine or arginine residues (R^2 group) did not inhibit T-L activity, although compound **4t**, with $R^1 = \text{NHC}_6\text{H}_4\text{OH}$, was a very poor inhibitor of T-L ($K_i = 126 \mu\text{M}$). All the molecules with positively charged lateral chains (**4l**, **4v**, **4aa–c**) inhibited the T-L active site ($K_i = 0.32 \mu\text{M}$ for **4aa** and $0.98 \mu\text{M}$ for **4ac**). Compound **4ac** inhibited with equal potency T-L ($K_i = 0.98 \mu\text{M}$) and CT-L activities ($K_i = 0.85 \mu\text{M}$), whereas ($K_{i,\text{CT-L}}/K_{i,\text{T-L}} = 2$ for **4ab** and 3 for **4aa**); PA activity was not inhibited (**4aa–c**). Compound **4ad**, with an $\text{NH}(\text{CH}_2)_4\text{NH}_2$ group at R^1 and not at R^2 , inhibited all three activities ($K_{i,\text{CT-L}}/K_{i,\text{T-L}} = 10$, $K_{i,\text{PA}} = 22.5 \mu\text{M}$). The protected lysine lateral chain $\text{NH}(\text{CH}_2)_4\text{NH-Boc}$ at position R^1 is unfavorable for inhibition (**4w–z**) except when $R^2 = i\text{Bu}$, since **4y** inhibited both CT-L and PA activities. The lateral chain of arginine was also recently introduced into endocyclic biphenyl ether compounds as a ligand of the S1 and S3 subsites.²⁰ The tyrosine hydroxyl group was protected in most compounds to facilitate their synthesis ($R^3 = \text{Me}$ or Bn). Its deprotection led to inhibitory activity (**4b** versus **4a**). Finally, the nature of the R^4 substituent may influence selectivity (**4ae** with $R^4 = \text{H}$ inhibited CT-L activity, while **4g** with $R^4 = \text{Boc}$ inhibited PA activity). Several of our linear mimics were moderate activators of proteasomes (over 1.2-fold).

We have designed and synthesized effective small proteasome inhibitors whose structures can be rationally modulated to act on all three active sites (**3h**, **4l**, **4v**, **4ad**), two active sites (**4aa–c** for CT-L and T-L; **3d**, **3e**, **3i**, **4b**, **4h**, **4q** for CT-L and PA), or only one active site (**1c**, **4f**, and **4g** for PA; **2b** for T-L) with K_i values of $0.32–84 \mu\text{M}$. Several compounds were more effective inhibitors of T-L than MG-132 (**3h**, **4v**, **4aa–d**) or equally inhibited PA activity (**4l**, **4v**) under our experimental conditions. Nevertheless, MG-132 is a better inhibitor of CT-L activity (12-fold better than **4aa**). The linear mimics **3** and **4** compare favorably with arecoline tripeptides,³² lipotripeptides having a large alkyl chain linked to the peptide N-terminus,³³ 5-methoxy-1-indanone dipeptide benzamides,³⁴ and the calpain I inhibitor Ac-LLN-H.^{12b} Moderate changes in the substituents of the TMC-95A macrocycle produced inhibitors with nanomolar K_i ,¹⁶ whereas greater alterations of the macrocycle structure to

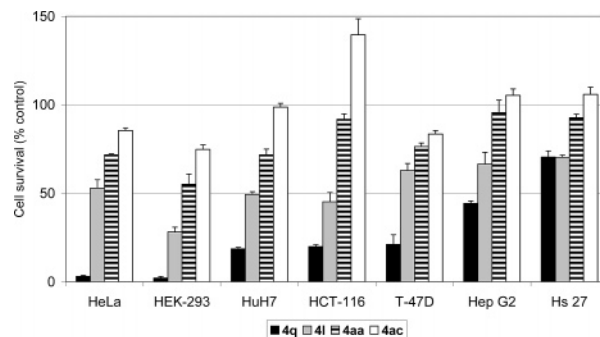


Figure 4. Cytotoxicity of some linear mimics for human cell lines. Cells were incubated with $50 \mu\text{M}$ **4q**, **4l**, **4aa**, or **4ac** for 48 h. Cell survival was then measured using an MTT assay.

facilitate synthesis gave inhibitors with activities similar to those of our linear molecules.^{17–19} Finally, we studied the metabolic stability of some linear mimics in RPMI culture medium containing fetal calf serum. The half-life of compound **3h** was 37 h and that of **4h** was 6.5 h, indicating reasonable stability.

The proteasome is an interesting new target for products designed to combat many diseases, particularly cancers.^{4,6} Targeting the T-L activity may be useful, since it is reported to be the rational choice for antitrypanosoma drugs.³⁵ Compounds **4l** and **4aa–d**, which inhibit T-L activity, may be molecules from which clinically useful noncovalent inhibitors of proteasomes can be developed. We tested the most potent in vitro inhibitors (**4l**, **4q**, **4aa**, and **4ac**) in six human tumor cell lines and in primary fibroblasts to determine their effects on cancer cells. The effects of these inhibitors increased in the order **4ac** < **4aa** < **4l** < **4q** (Figure 4). Compound **4ac** had negligible inhibitory effects and even slightly stimulated HCT-116 cells. But all the cell lines were sensitive to incubation with $50 \mu\text{M}$ **4q** for 48 h. Two of them (HeLa and HEK-293) were killed, while the growth of three others was severely inhibited (HuH7, HCT 116, T-47D). One cell line (Hep G2) was significantly resistant to **4q**. The less sensitive cells (primary fibroblasts Hs 27) were the only nontumoral cells tested. Compound **4q** had an IC_{50} of $15 \pm 5 \mu\text{M}$ on HeLa cells, about 500-fold higher than that of MG132 tested under the same conditions (data not shown) and close to that of TMC-95A for human tumor cell lines (HCT-116, $\text{IC}_{50} = 4.4 \mu\text{M}$, and HL-60, $\text{IC}_{50} = 9.8 \mu\text{M}$).¹¹ Cell cycle analysis of synchronized HeLa cells showed that progression through the cell cycle phases was slower in cells incubated with **4q** than in control untreated cells (data not shown).

Conclusion

We have prepared and tested new reversible noncovalent inhibitors of proteasomes using TMC-95A as template. They differ dramatically from the parent molecule TMC-95A, since they lack the biaryl linkage responsible for a constrained conformation. They also differ from the traditional electrophilic peptide inhibitors of proteasome (peptide boronates, peptide aldehydes, α,β -epoxyketones) in that they have no reactive group ("warhead") that could react with the catalytic $\text{O}^\gamma\text{-Thr1}$ of the proteasome. Hence, they are all readily synthesized and their skeleton can be used to introduce structural variations to orientate selectivity for one or more of the three catalytic sites. The linear scaffold is suitable for an optimized display of groups interacting with each binding subsite. Analysis of the roles of R^1 and R^2 substituents susceptible to act as P1 and P3 residues indicates (a) the favorable effect of an electron-rich aromatic

substituent at R¹ position (NHBn, NHC₆H₄OH) or its total absence with a free carboxylic C-end, (b) an orientation toward T-L activity with lysine and arginine lateral chains at position R² or even at position R¹, (c) a possible orientation toward specific inhibition of PA activity. They are significant inhibitors in vitro and in cell tumor lines and are metabolically stable. These versatile compounds open a new avenue for the development of new low molecular weight and noncovalently binding proteasome inhibitors that act selectively on one or more of the three proteasome activities.

Experimental Section

Chemistry. The syntheses of the more active compounds are indicated below. For description of general methods and preparation of the other compounds, see Supporting Information.

***N*-Boc-Tyr(Bn,3-iodo)-Ala-Trp(7-bromo)-OH (3h).** A solution of *N*-Boc-Tyr(Bn,3-iodo)-Ala-Trp(7-bromo)-OMe **3c** (85.5 mg, 0.100 mmol) in THF (0.4 mL) was treated at 0 °C by 1 M aqueous NaOH (0.12 mL, 0.12 mmol). After 5 h at room temperature, 1 M aqueous HCl was added (0.36 mL, 0.36 mmol). The resulting mixture was diluted by water and extracted by CH₂Cl₂ (3 × 10 mL). After drying of the organic phase over Na₂SO₄ and evaporation of the solvent, the residue was subjected to flash chromatography on silica gel (2% MeOH/CH₂Cl₂) to afford remaining *N*-Boc-Tyr(Bn, 3-iodo)-Ala-Trp(7-bromo)-OMe **3c** (10.13 mg, 12%) and *N*-Boc-Tyr(Bn, 3-iodo)-Ala-Trp(7-bromo)-OH **3h** (58.3 mg, 70%, corrected yield 82%) as a white amorphous solid. ¹H NMR (200 MHz, CDCl₃) δ 0.9 (d, *J* = 6.4 Hz, 3H, CH₃), 1.42 (s, 9H, (CH₃)₃), 2.87 (m, CH₂ Tyr), 3.32 (m, 2H, CH₂ Trp), 4.40 (m, 1H, CH Tyr), 4.52 (m, 1H CH Ala), 4.85 (m, 1H, CH Trp), 5.06 (s, 2H, CH₂O), 5.16 (broad d, *J* = 7.6 Hz, 1H, NHBoc), 6.71 (d, *J* = 8 Hz, 1H, H₅ Tyr), 6.91 – 7.58 (m, 14 H, aromatic H and NH), 8.68 (s, 1H, NHind). ¹³C NMR (75 MHz, acetone-*d*₆) δ 19.4 (CH₃ Ala), 29.1 (CH₂ Trp), 29.5 ((CH₃)₃), 38.3 (CH₂ Tyr), 50.4 (CH Ala), 54.7 (CH Trp), 57.4 (CH Tyr), 72.3 (CH₂O), 80.5 (C(CH₃)₃), 87.6 (C₃ Tyr), 106.1 (C₇ Trp), 114.3 (CH ar), 120.0 (CH ar), 120.7 (Car), 122.0 (CH ar), 125.6 (CH ar), 126.7 (Car), 129.0 (CH ar), 129.5 (CH ar), 130.2 (CH ar), 131.3 (Car), 132.7 (CH ar), 134.2 (Car), 136.5 (Car), 138.9 (Car), 142.0 (CH ar), 157.3, 157.8 (C₄ Tyr or CO Boc), 172.9, 173.7, 174.1 (2 CO amide, CO acid). HRMS (ESI) calcd for C₃₅H₃₈⁷⁹BrIN₄O₇Na [(M + Na)⁺] 855.0866, found 855.0896. Anal. (C₃₅H₃₈BrIN₄O₇·2H₂O) C, H, N: calcd, 6.44; found, 5.73. HPLC homogeneity: >97% (system A, *t*_R = 13); >99% (system B, *t*_R = 17.8).

***N*-Boc-Tyr-Ala-Trp-OMe (4b).** *N*-Boc-Tyr(Bn)-Ala-Trp-OMe **4a** (119 mg, 0.185 mmol) in solution in MeOH (4 mL) was hydrogenated overnight at atmospheric pressure in the presence of 10% Pd on charcoal (30 mg). After filtration, evaporation of the solvent, and trituration with ether, *N*-Boc-Tyr-Ala-Trp-OMe (77 mg, 76%) was obtained as a solid. ¹H NMR (300 MHz, DMSO-*d*₆) δ 1.19 (d, *J* = 7 Hz, 3H, CH₃), 1.29 (s, 9H, (CH₃)₃), 2.55 and 2.80 (ABX system, 2H, CH₂β), 3.13 and 3.16 (ABX system, 2H, CH₂ β), 3.55 (s, 3H, OCH₃), 4.05 (m, 1H, CHα), 4.35 (m, 1H, CHα), 4.50 (m, 1H, CHα), 6.63 (d, *J* = 8.3 Hz, 2H), 6.83 (d, *J* = 8.6 Hz, 1H), 7.03 (m, 4H), 7.16 (d, *J* = 2.1 Hz, 1H), 7.34 (d, *J* = 7.9 Hz, 1H), 7.47 (d, *J* = 7.8 Hz, 1H), 7.92 (d, *J* = 7.4 Hz, 1H, NH), 8.32 (d, *J* = 7.3 Hz, 1H, NH), 9.14 (s, 1H, OH), 10.86 (s, 1NH). ¹³C NMR (75 MHz, DMSO-*d*₆) δ 18.4 (CH₃), 26.9 (CH₂ Trp), 28.1 ((CH₃)₃), 36.4 (CH₂ Tyr), 47.8, 51.7, 53.0, 55.9 (CHα Ala, Tyr, Trp or OCH₃), 77.9 (C(CH₃)₃), 109.1 (aromatic C), 111.4, 114.8, 117.9, 118.4, 120.9, 123.7 (aromatic CH), 127.0, 128.2 (aromatic C), 130.0 (aromatic CH), 136.0 (aromatic C), 155.2, 156.6 (Car-O or CO carbamate), 171.4, 172.0, 172.2 (2 CO amide or CO ester). HRMS (ESI) calcd for C₂₉H₃₆N₄O₇Na [(M + Na)⁺] 575.2482, found 575.2480. Anal. (C₂₉H₃₆N₄O₇·H₂O) C, H, N.

***N*-Boc-Tyr-Arg-Trp-NHCH₂Ph (4l).** A solution of *N*-Boc-Tyr(Bn)-Arg(Z₂)-Trp-NHCH₂Ph **4k** (86.15 mg, 0.0804 mmol) in MeOH/DMF (1.4 mL, 1/0.4) was hydrogenated at atmospheric

pressure over 10% Pd on charcoal (9.14 mg) for 18 h. The mixture was filtered over a pad of Celite and concentrated. After the mixture was washed with ether, the product was afforded as a white solid (46.55 mg, 81%). ¹H NMR (300 MHz, DMSO-*d*₆) δ 1.09–1.63 (m, 4H, (CH₂)₂ Arg), 1.30 (s, 9 H, (CH₃)₃), 2.62–3.14 (m, 6H), 4.05 (m, 1H, CHα), 4.23 (m, 3H, CH₂ Ph and CHα), 4.56 (m, 1H, CHα), 6.60 (m, 2H, aromatic CH), 6.96–7.58 (m, 11H, aromatic H), 7.96 (m, 1H, aromatic H). ¹³C NMR (75 MHz, CD₃OD) δ 25.9 (CH₂ γ Lys), 28.7 (CH₃ Boc), 28.9, 29.9 (CH₂ Trp or CH₂ β Lys), 38.1 (CH₂ Tyr), 41.9 (CH₂N Lys), 44.2 (CH₂NPh), 54.3, 55.9, 57.9 (CH α Lys or Trp or Tyr), 80.9 (C Boc), 110.7 (Car), 112.4, 118.0, 119.4, 119.9, 122.5, 124.6 (CH ar), 126.0 (Car), 128.1, 128.4 (CH ar), 128.8 (Car), 129.4, 131.3 (CH ar), 138.0, 139.4 (Car), 157.9, 158.6, 161.5 (C=N or CarO or NCOO), 173.3, 173.8, 175.0 (CONH). HRMS (ESI) calcd for C₃₈H₄₉N₈O₆ [(M + H)⁺] 713.3775, found 713.3778. HPLC homogeneity: >95% (system A, *t*_R = 10.1); >95% (system B, *t*_R = 13.8).

***N*-Boc-Tyr(Bn)-Ala-Trp-NH(4-OH)Ph (4q).** To a solution of *N*-Boc-Tyr(Bn)-Ala-OH (106.4 mg, 0.24 mmol) in CH₂Cl₂/DMF (1.5 mL, 1/1) at 0 °C were successively added EDC (53.8 mg, 0.28 mmol), HOBt (37.9 mg, 0.28 mmol), and Trp-NHPhOH **6g** (75 mg, 0.254 mmol). The resulting mixture was allowed to warm to room temperature overnight. The solvent was evaporated, and the crude was triturated with water. After filtration, the solid was collected and washed with Et₂O to afford a pale-brown solid (72.8 mg, 42%). ¹H NMR (300 MHz, DMSO-*d*₆) δ 1.21 (d, *J* = 6.7 Hz, 3H, CH₃), 1.28 (s, 9H, (CH₃)₃), 2.62–3.21 (m, 4H, CH₂ Tyr, CH₂ Trp), 4.1 (m, 1H, CHα), 4.32 (m, 1H, CHα), 4.64 (m, 1H, CHα), 5.02 (s, 2H, CH₂ (Bn)), 6.66 (d, *J* = 8.4 Hz, 1H), 6.87–7.39 (m, 17H), 7.6 (d, *J* = 7 Hz, 1H), 8 (d, *J* = 6.9 Hz, 1H), 8.1 (d, *J* = 7.1 Hz, 1H), 9.18 (s, 1 NH), 9.74 (s, 1 NH), 10.8 (s, 1H, NH). ¹³C NMR (75 MHz, DMSO-*d*₆) δ 18.2 (CH₃), 27.8 (CH₂ Trp), 28 ((CH₃)₃), 36.2 (CH₂ Tyr), 48.1, 53.9, 55.7 (CHα Ala, Tyr, Trp), 69 (CH₂ (Bn)), 78 (C(CH₃)₃), 109.6, 111.1, 114.2, 114.9, 118.1, 118.4, 120.7, 121, 123.4, 127.2, 127.5, 127.6, 128.3, 130.1, 130.2, 130.3, 135.9, 137.1 (24 aromatic C), 153.3, 155.2, 156.7 (2 Car-O, CO carbamate), 169.2, 171.4, 171.9 (3 CO amide). HRMS (ESI) calcd for C₄₁H₄₅N₅O₇Na [(M + Na)⁺] 742.3217, found 742.3223. Anal. (C₄₁H₄₅N₅O₇·2H₂O) C, H, N.

***N*-Boc-Tyr-Arg-Trp-NH(4-OH)Ph (4v).** The same procedure as for **4l** was used, using *N*-Boc-Tyr(Bn)-Arg(Z₂)-Trp-NH(4-OH)-Ph **4u** (60.81 mg, 0.0567 mmol) and 10% Pd on charcoal (6.43 mg) in MeOH/DMF (0.8 mL, 7/1) and affording after washing with ether *N*-Boc-Tyr-Arg-Trp-NH(4-OH)Ph as a white solid (34.89 mg, 86%). ¹H NMR (300 MHz, DMSO-*d*₆) δ 1.23–1.65 (m, 4H, (CH₂)₂ Arg), 1.31 (s, 9 H, (CH₃)₃), 2.73–3.17 (m, 6H), 4.09 (m, 1H, CHα), 4.28 (m, 1H, CHα), 4.63 (m, 1H, CHα), 6.59 (m, 3H, aromatic CH), 6.92–7.31 (m, 7H, aromatic H), 7.57 (d, *J* = 7.6 Hz, 1H, aromatic H). ¹³C NMR (75 MHz, CD₃OD) δ 26.1 (CH₂ γ Lys), 28.7 (CH₃ Boc), 26.7, 28.9 (CH₂ Trp or CH₂ β Lys), 34.8 (CH₂ Tyr), 41.9 (CH₂N Lys), 53.7, 56.4, 57.6 (CH α Lys or Trp or Tyr), 80.8 (C Boc), 110.6 (Car), 112.3, 116.9 (CH ar), 117.2 (C ar), 119.4, 119.9, 122.4, 124.1, 124.6 (CH ar), 128.7 (Car), 131.3 (CH ar), 138.0 (Car), 157.8, 158.4 (C=N or CarO or NCOO), 172.2, 173.3, 174.7 (CONH). HRMS (ESI) calcd for C₃₇H₄₇N₈O₇ [(M + H)⁺] 715.3568, found 715.3572. HPLC homogeneity: >95% (system A, *t*_R = 9.8); >95% (system B, *t*_R = 13.2).

Tyr(Bn)-Lys-Trp-NHCH₂Ph (4aa). *N*-Boc-Tyr(Bn)-Lys(Boc)-Trp-NHCH₂Ph·2H₂O (80.23 mg, 0.0881 mmol) was reacted with 3 M anhydrous HCl in MeOH (1.5 mL) overnight. After solvent evaporation and washing of the residue with ether, a solid was obtained (33.3 mg). Purification of this crude product by MPLC over RP silica (C18, 3 g) afforded after lyophilization Tyr(Bn)-Lys-Trp-NHCH₂Ph·3HCl·2H₂O as a white solid (17 mg, 24%). ¹H NMR (300 MHz, CD₃OD) δ 1.30 (m, 2H, CH₂ Lys), 1.49–1.72 (m, 4H, CH₂ Lys), 2.73–2.83 (m, 3H, CH of ABX system and CH₂ Lys), 2.95–3.21 (m, 3H, CH of ABX system and CH₂), 4.00 (dd, *J* = 7.5 Hz, *J* = 6.0 Hz, 1H, CHα), 4.11 and 4.20 (AB system, *J* = 15 Hz, 2H, NCH₂Ph), 4.29 (t, *J* = 7 Hz, 1H, CHα Lys), 4.58 (t, *J* = 7.2 Hz, 1H, CHα), 4.89 (m, 2H, CH₂ (Bn)), 6.80 (d, *J* = 8.6 Hz, 2H), 6.89–7.30 (m, 15H), 7.54 (d, *J* = 7.6 Hz,

1H). ¹³C NMR (75 MHz, CD₃OD) δ 23.5 (CH₂), 28.1 (CH₂), 29.3 (CH₂), 32.5 (CH₂), 37.8 (CH₂), 40.4 (CH₂), 44.1 (NCH₂Ph), 54.7 (CH), 55.6 (CH), 55.9 (CH), 70.9 (CH₂), 110.6 (C), 112.4 (CH), 116.4 (CH), 119.4 (CH), 120.0 (CH), 122.5 (CH), 124.8 (CH), 127.5 (C), 128.1 (CH), 128.4 (C), 128.5 (CH), 128.8 (C), 128.9 (CH), 129.4 (CH), 129.5 (CH), 131.7 (CH), 138.1 (C), 138.6 (C), 139.4 (C), 159.8 (C), 169.9 (CO), 172.9 (CO), 173.7 (CO). HRMS (LSIMS with Cs⁺) calcd for C₄₀H₄₇N₆O₄ [M + H⁺] 675.3659, found 675.3659. Anal. (C₄₀H₄₆N₆O₄·1.5H₂O·3HCl) C, H, N.

Tyr(Bn)-Lys-Trp-NHPh (4ab). *N*-Boc-Tyr(Bn)-Lys(Boc)-Trp-NHPh·1.5H₂O (91.88 mg, 0.103 mmol) was reacted with 3 M anhydrous HCl in MeOH (1.5 mL) for 3 h. After solvent evaporation and washing of the residue with ether, a solid was obtained (68.3 mg). Purification of a portion of this crude product (37.8 mg) by MPLC over RP silica (C18, 3 g) afforded after lyophilization Tyr(Bn)-Lys-Trp-NHPh·3HCl·2H₂O as a white solid (17.2 mg, 38%). ¹H NMR (300 MHz, D₂O) δ 1.20 (m, 2H, CH₂ Lys), 1.53 (m, 4H, CH₂ Lys), 2.78 (t, *J* = 7.8 Hz, 2H, CH₂ Lys), 2.85 (dd, *J* = 13.5 Hz, *J* = 6.8 Hz, 1H), 2.98 (dd, *J* = 13.5 Hz, *J* = 6.8 Hz, 1H), 3.42 (m, 2H, CH₂), 4.08 (t, *J* = 6.8 Hz, 1H, CHα), 4.27 (t, *J* = 7 Hz, 1H, CHα Lys), 4.56 (t, *J* = 6.4 Hz, 1H, CHα), 4.84 (s, 2H, CH₂ (Bn)), 6.75 (d, *J* = 8.45 Hz, 2H), 6.92 (d, *J* = 8.45 Hz, 2H), 7.01–7.34 (m, 14H), 7.58 (d, *J* = 7.3 Hz, 1H). ¹³C NMR (75 MHz, CD₃OD) δ 23.5 (CH₂), 28.1 (CH₂), 29.3 (CH₂), 32.5 (CH₂), 37.8 (CH₂), 40.4 (CH₂), 54.7 (CH), 55.6 (CH), 56.3 (CH), 70.9 (CH₂), 110.6 (C), 112.4 (CH), 116.5 (CH), 119.5 (CH), 120.0 (CH), 121.7 (CH), 122.5 (CH), 124.8 (CH), 125.5 (C), 127.5 (CH), 128.5 (C), 128.8 (CH), 128.9 (CH), 129.5 (CH), 129.8 (CH), 131.73 (CH), 138.0 (C), 138.6 (C), 139.2 (C), 159.8 (C), 169.9 (CO), 172.2 (CO), 173.0 (CO). HRMS (LSIMS with Cs⁺) calcd for C₃₉H₄₅N₆O₄ [M + H⁺] 661.3502, found 661.3503. Anal. (C₃₉H₄₄N₆O₄·2H₂O·3HCl) C, H, N.

Tyr(Bn)-Lys-Trp-NH(4-OH)Ph (4ac). *N*-Boc-Tyr(Bn)-Lys(Boc)-Trp-NH(4-OH)Ph·3H₂O (80.04 mg, 0.0859 mmol) was reacted with 3 M anhydrous HCl in MeOH (1.5 mL) overnight. After solvent evaporation and washing of the residue with ether, a solid was obtained (61.5 mg). Purification of this crude product by MPLC over RP silica (C18, 6 g) afforded after lyophilization Tyr(Bn)-Lys-Trp-NH(4-OH)Ph·3HCl·2H₂O as a white solid (60.7 mg, 86%). ¹H NMR (300 MHz, D₂O) δ 1.20 (m, 2H, CH₂ Lys), 1.52 (m, 4H, CH₂ Lys), 2.78 (t, *J* = 7.5 Hz, 2H, NCH₂ Lys), 2.84 (dd, *J* = 14.5 Hz, *J* = 7.5 Hz, 1H), 2.97 (dd, *J* = 14.5 Hz, *J* = 5 Hz, 1H), 3.21 (m, 2H, CH₂), 4.08 (t, *J* = 6.5 Hz, 1H, CHα), 4.25 (t, *J* = 7 Hz, 1H, CHα), 4.50 (t, *J* = 8 Hz, 1H, CHα), 4.80 (s, 2H, CH₂ (Bn)), 6.67–7.32 (m, 17H), 7.56 (d, *J* = 8 Hz, 1H). ¹³C NMR (50 MHz, CD₃OD) δ 23.4 (CH₂), 28.0 (CH₂), 29.3 (CH₂), 32.5 (CH₂), 37.8 (CH₂), 40.4 (CH₂), 54.7 (CH), 55.5 (CH), 56.1 (CH), 70.9 (CH₂), 110.6, 112.3, 116.1, 116.4, 119.4, 119.9, 122.5, 123.8, 124.8, 127.4, 128.5, 128.7, 128.8, 129.5, 130.9, 131.7, 138.0, 138.5, 155.7, 159.8, 169.8 (CO), 171.9 (CO), 172.9 (CO). HRMS (LSIMS with Cs⁺) calcd for C₃₉H₄₅N₆O₅ [M + H⁺] 677.3451, found 677.3440. Anal. (C₃₉H₄₄N₆O₅·2H₂O·3HCl) C, H, N.

Tyr(Bn)-Leu-Trp-NH(CH₂)₄NH₂ (4ad). *N*-Boc-Tyr(Bn)-Leu-Trp-NH(CH₂)₄-NH₂·0.5H₂O (85.52 mg, 0.100 mmol) was reacted with 3 M anhydrous HCl in MeOH (1.5 mL) overnight. After solvent evaporation and washing of the residue with ether, a solid was obtained (28 mg). Purification of a portion of this crude product (14 mg) by MPLC over RP silica (C18, 3 g) afforded after lyophilization Tyr(Bn)-Leu-Trp-NH(CH₂)₄NH₂·3HCl·2H₂O as a white solid (10.3 mg, 26%). ¹H NMR (300 MHz, D₂O) δ 0.75 (d, *J* = 5.7 Hz, 3H, CH₃ Leu), 0.80 (d, *J* = 5.7 Hz, 3H, CH₃ Leu), 1.20 (m, 4H, CH₂), 1.38 (m, 3H, CH₂ and CH), 2.70 (t, *J* = 6.7 Hz, 2H, CH₂), 2.81–3.11 (m, 6H), 4.06 (t, *J* = 7.5 Hz, 1H, CHα), 4.27 (t, *J* = 7.2 Hz, 1H, CHα Lys), 4.40 (t, *J* = 7.2 Hz, 1H, CHα), 4.81 (m, 2H, OCH₂), 6.73 (d, *J* = 8.5 Hz, 2H), 6.90 (d, *J* = 8.5 Hz, 2H), 7.01–7.35 (m, 8H), 7.56 (d, *J* = 7.1 Hz, 2H). ¹³C NMR (75 MHz, D₂O) δ 22.0 (CH₃), 22.5 (CH₃), 24.5 (CH₂), 24.9 (CH), 25.8 (CH₂), 28.0 (CH₂), 36.6 (CH₂), 39.1 (CH₂), 39.6 (CH₂), 40.7 (CH₂), 52.8 (CH), 54.8 (CH), 55.6 (CH), 70.9 (CH₂), 109.6 (C), 112.6 (CH), 116.2 (CH), 119.1 (CH), 120.1 (CH), 122.6 (CH), 125.1 (CH), 126.9 (C), 127.6 (C), 128.6 (CH), 129.1 (CH), 129.5 (CH),

131.3 (CH), 136.9 (C), 137.0 (C), 158.1 (C), 169.2 (CO), 173.3 (CO), 173.4 (CO). HRMS (LSIMS with Cs⁺) calcd for C₃₇H₄₉N₆O₄ [M + H⁺] 641.3815, found 641.3806. Anal. (C₃₇H₄₈N₆O₄·2.5H₂O·3HCl) C, H, N.

Tyr(Bn)-Ala-Trp-NHCH₂Ph (4ae). *N*-Boc-Tyr(Bn)-Ala-Trp-NHCH₂Ph **4g** (77.55 mg, 0.108 mmol) in THF (0.8 mL) was reacted with 3 M anhydrous HCl in MeOH (0.2 mL) overnight. After solvent evaporation, purification of the product by MPLC over RP silica (C18, 6 g) afforded after lyophilization Tyr(Bn)-Ala-Trp-NHCH₂Ph·2HCl·1.5H₂O as a white powder (49.3 mg, 64%). ¹H NMR (300 MHz, DMSO-*d*₆) δ 1.23 (d, *J* = 6.9 Hz, 3H, CH₃), 2.80 (m, 1H, CH₂), 3.01 (m, 2H, CH₂), 3.14 (dd, *J* = 14.4 Hz, 6.9 Hz, 1H, CH₂), 3.96 (m, 1H, CHα), 4.23 (m, 2H, NCH₂), 4.43 (quint, *J* = 7.1 Hz, 1H, CHα), 4.61 (q, *J* = 7.5 Hz 1H, CHα), 4.96 (s, 2H, CH₂ (Bn)), 6.89–7.40 (m, 19 aromatic H), 7.63 (d, *J* = 7.8 Hz, 1H), 7.97 (m, 3H), 8.25 (d, *J* = 7.8 Hz, 1H), 8.47 (t, *J* = 6 Hz, 1H), 8.66 (d, *J* = 7.0 Hz, 1H), 10.86 (s, 1NH). ¹³C NMR (75 MHz, CD₃OD) δ 17.9 (CH₃), 29.2 (CH₂), 37.5 (CH₂), 44.0 (NCH₂-Ph), 50.5 (CH), 55.4 (CH), 55.7 (CH), 70.7 (CH₂), 110.5 (C), 112.3 (CH), 116.3 (CH), 119.3 (CH), 119.8 (CH), 122.4 (CH), 124.7 (C), 127.3 (C), 127.9 (CH), 128.2 (CH), 128.3 (CH), 128.7 (CH), 129.3 (CH), 129.3 (CH), 131.6 (CH), 137.9 (C), 138.4 (C), 139.2 (C), 159.7 (C), 169.4 (CO), 173.3 (CO), 173.7 (CO). HRMS (ESI) calcd for C₃₇H₄₀N₅O₄ [M + H⁺] 618.3080, found 618.3106. Anal. Calcd for C₃₇H₃₉N₅O₄·1.5H₂O·2HCl: C, 61.92; H, 6.18; N, 9.76. Found: C, 62.14; H, 6.17; N, 9.80.

Enzyme Studies. Rabbit reticulocyte 20S proteasome was obtained from Boston Biochem, Cambridge, MA. The fluorogenic substrates Suc-LLVY-AMC, Boc-LRR-AMC, and Z-LLE-βNA used to measure the proteasome CT-L, T-L, and PA activities were purchased from Bachem (France). Other reagents and solvents were purchased from commercial sources. Fluorescence was measured using a BMG Fluostar microplate reader.

Enzyme and Inhibition Assays. Enzyme activities were determined by monitoring the hydrolysis of the appropriate fluorogenic substrate ($\lambda_{\text{exc}} = 360$ and $\lambda_{\text{em}} = 465$ nm for AMC substrates; $\lambda_{\text{exc}} = 340$ and $\lambda_{\text{em}} = 405$ nm for the βNA substrate) for 1 h at 37 °C in the presence of untreated (control) or proteasome that had been incubated with 0.1–100 μM test compounds. Substrates and compounds were previously dissolved in DMSO, with the final solvent concentration kept constant at 3% (v/v). The buffers were (pH 7.5) 20 mM Tris, 1 mM DTT, 10% glycerol, 0.02% (w/v) SDS for CT-L and PA activities and 20 mM Tris, 1 mM DTT, 10% glycerol for T-L activity. Initial rates determined in control experiments (V_0) were considered to be 100% of the peptidase activity; initial rates (V_i) that were above 100% in the presence of a test compound were considered to be activations (expressed as activation factor), while initial rates below 100% were considered to be inhibitions. The inhibitory activities of compounds are expressed as K_i . The inhibition constants K_i were determined using the equation $V_i/V_0 = 1/(1 + [I]/K_{i(\text{app})})$ with $K_{i(\text{app})} = K_i(1 + [S]/K_m)$ or using the equation $\text{IC}_{50} = K_i(1 + [S]/K_m)$. The IC₅₀ values (inhibitor concentrations giving 50% inhibition) were obtained by plotting the percent inhibition against inhibitor concentration and fitting the experimental data to the equation % inhibition = 100·[I]₀/(IC₅₀ + [I]₀) or, in few cases (compounds **3h** and T-L activities and **4b**), to the equation % inhibition = 100 [I]₀^{*n*_H}/(IC₅₀^{*n*_H} + [I]₀^{*n*_H}) where *n*_H is the Hill number.

Evaluation of Metabolic Stability. The breakdown of the inhibitors was studied by incubating them in RPMI culture medium containing 20% fetal calf serum, at 37 °C for up to 2 days. The reaction was terminated by adding ethanol, and the mixture was separated by centrifugation at 4 °C (10 000 rpm for 10 min). Aliquots (20 μL) of the supernatant were injected onto the RP-HPLC column. The breakdown half-life was obtained by a least-squares linear regression analysis of a plot of the log [I] versus time using a minimum of five points.

Cell Culture and Cytotoxicity Assays. HeLa (cervical carcinoma), T-47D (mammary carcinoma), HEK-293 (epithelial kidney), HuH7 (hepatocarcinoma), Hep G2 (hepatoblastoma), HCT-116 (colorectal carcinoma) human cell lines, and Hs 27 primary

fibroblasts were obtained from the American Type Culture Collection (Manassas, VA). The cells were grown in DMEM (HeLa, T-47D, Hs 27), MEM (HEK-293, HuH7, Hep G2), or McCoy (HCT-116) media supplemented with 10% fetal bovine serum in a humidified atmosphere of 5% CO₂ and 95% air.

The cells were incubated with varying concentrations of proteasome inhibitors, and cell survival was assessed at 37 °C by measuring the ability of the various cell lines to metabolize 3-(4,5-dimethyl-diazol-2-yl)-2,5-diphenyl-tetrazolium bromide (MTT). The 5 × 10³ cells in 100 μL of culture medium were grown in triplicate for 48 h in 96-well plates, with and without 50 μM inhibitors. MTT solution (15 μL) was then added to each well, and the samples were treated according to the manufacturer's protocol (Promega). The results are expressed relative to the control values of cells treated with the DMSO alone.

Acknowledgment. We thank the "Ligue Nationale contre le Cancer" and the "Association Française contre les Myopathies" (AFM) for financial support. N.B. is supported by a fellowship from AFM. A.F.-B. thanks the Ministère de la Jeunesse, de l'Éducation Nationale et de la Recherche for a doctoral fellowship. The English text was edited by Dr. Owen Parkes.

Supporting Information Available: General and experimental chemical procedures, characterization data for all new compounds, and elemental analysis data. This material is available free of charge via the Internet at <http://pubs.acs.org>.

References

- (1) (a) Coux, O.; Tanaka, K.; Goldberg, A. L. Structure and functions of the 20S and 26S proteasomes *Annu. Rev. Biochem.* **1996**, *65*, 801–847. (b) Ciechanover, A. The ubiquitin–proteasome pathway: on protein death and cell life. *EMBO J.* **1998**, *17*, 7151–7160.
- (2) Rock, K.; York, I. A.; Goldberg, A. L. Post-proteasomal antigen processing for major histocompatibility complex class I presentation. *Nat. Immunol.* **2004**, *5*, 670–677.
- (3) (a) Goldberg, A. L.; Rock, K. Not just research tools—proteasome inhibitors offer therapeutic promise. *Nat. Med.* **2002**, *8*, 338–340. (b) Myung, J.; Kim, K. B.; Crews, C. M. The ubiquitin–proteasome pathway and proteasome inhibitors. *Med. Res. Rev.* **2001**, *21*, 245–273.
- (4) Adams, J., Ed. *Proteasome Inhibitors in Cancer Therapy*; Humana Press: Totowa, NJ, 2004.
- (5) Kisselev, A. F.; Goldberg, A. L. Proteasome inhibitors: from research tools to drug candidates. *Chem. Biol.* **2001**, *8*, 739–758.
- (6) Garcia-Echeverria, C. Peptide and peptide-like modulators of 20S proteasome enzymatic activity in cancer cells. *Int. J. Pept. Res. Ther.* **2006**, *12*, 49–64.
- (7) Groll, M.; Huber, R.; Potts, B. C. M. Crystal structures of salinosporamide A (NPI-0052) and B (NPI-0047) in complex with the 20S proteasome reveal important consequences of β-lactone ring opening and a mechanism for irreversible binding. *J. Am. Chem. Soc.* **2006**, *128*, 5136–5141 and references cited therein.
- (8) Schmidke, G.; Holzthutter, H. G.; Bogyo, M.; Kairies, N.; Groll, M.; de Giuli, R.; Emch, S.; Groettrup, M. How an inhibitor of the HIV-1 protease modulates proteasome activity. *J. Biol. Chem.* **1999**, *274*, 35734–35740.
- (9) (a) Furet, P.; Imbach, P.; Noorani, M.; Koeppler, J.; Laumen, K.; Lang, M.; Guagnano, V.; Fuerst, P.; Roesel, J.; Zimmermann, J.; Garcia-Echeverria, C. Entry into a new class of potent proteasome inhibitors having high antiproliferative activity by structure-based design. *J. Med. Chem.* **2004**, *47*, 4810–4813. (b) Garcia-Echeverria, C.; Imbach, P.; France, D.; Furst, P.; Lang, M.; Noorani, A. M.; Scholz, D.; Zimmermann, J.; Furet, P. A new structural class of selective and non-covalent inhibitors of the chymotrypsin-like activity of the 20S proteasome. *Bioorg. Med. Chem. Lett.* **2001**, *11*, 1317–1319. (c) Furet, P.; Imbach, P.; Fuerst, P.; Lang, M.; Noorani, M.; Zimmermann, J.; Garcia-Echeverria, C. Structure-based optimisation of 2-aminobenzylstatin derivatives: potent and selective inhibitors of the chymotrypsin-like activity of the human 20S proteasome. *Bioorg. Med. Chem. Lett.* **2002**, *12*, 1331–1334.
- (10) Kohno, J.; Koguchi, Y.; Nishio, M.; Nakao, K.; Kuroda, M.; Shimizu, R.; Ohnuki, T.; Komatsubara, S. Structures of TMC-95A-D: novel proteasome inhibitors from *Apiospora montagnei* sacc. TC 1093. *J. Org. Chem.* **2000**, *65*, 990–995.
- (11) Koguchi, Y.; Kohno, J.; Nishio, M.; Takahashi, K.; Okuda, T.; Ohnuki, T.; Komatsubara, S. TMC-95A, B, C, and D, novel proteasome inhibitors produced by *Apiospora montagnei* Sacc. TC 1093. Taxonomy, production, isolation, and biological activities. *J. Antibiot.* **2000**, *53*, 105–109.
- (12) (a) Groll, M.; Koguchi, Y.; Huber, R.; Kohno, J. Crystal structure of the 20 S proteasome:TMC-95A complex: a non-covalent proteasome inhibitor. *J. Mol. Biol.* **2001**, *311*, 543–548. (b) Kaiser, M.; Groll, M.; Siciliano, C.; Assfalg-Machleidt, I.; Weyher, E.; Kohno, J.; Milbradt, A. G.; Renner, C.; Huber, R.; Moroder, L. Binding mode of TMC-95A analogues to eukaryotic 20S proteasome. *ChemBioChem* **2004**, *5* (9), 1256–1266.
- (13) (a) Lin, S.; Danishefsky, S. J. The total synthesis of proteasome inhibitors TMC-95A and TMC-95B: discovery of a new method to generate cis-propenyl amides. *Angew. Chem., Int. Ed.* **2002**, *41*, 512–515. (b) Lin, S.; Yang, Z. Q.; Kwok, B. H.; Koldobskiy, M.; Crews, C. M.; Danishefsky, S. J. Total synthesis of TMC-95A and -B via a new reaction leading to Z-enamides. Some preliminary findings as to SAR. *J. Am. Chem. Soc.* **2004**, *126*, 6347–6355.
- (14) Inoue, M.; Sakazaki, H.; Furuyama, H.; Hiram, M. Total synthesis of TMC-95A. *Angew. Chem., Int. Ed.* **2003**, *42*, 2654–2657.
- (15) (a) Albrecht, B. K.; Williams, R. M. A concise, total synthesis of the TMC-95A/B proteasome inhibitors. *Proc. Natl. Acad. Sci. U.S.A.* **2004**, *101*, 11949–11954. (b) Albrecht, B. K.; Williams, R. M. A concise formal total synthesis of TMC-95A/B proteasome inhibitors. *Org. Lett.* **2003**, *5* (2), 197–200.
- (16) Yang, Z.-Q.; Kwok, B. H. B.; Lin, S.; Koldobskiy, M. A.; Crews, C. M.; Danishefsky, S. J. Simplified synthetic TMC-95A/B analogues retain the potency of proteasome inhibitory activity. *ChemBioChem* **2003**, *4*, 508–513.
- (17) Kaiser, M.; Groll, M.; Renner, C.; Huber, R.; Moroder, L. The core structure of TMC-95A is a promising lead for reversible proteasome inhibition. *Angew. Chem., Int. Ed.* **2002**, *41*, 780–783.
- (18) Kaiser, M.; Siciliano, C.; Assfalg-Machleidt, I.; Groll, M.; Milbradt, A. G.; Moroder, L. Synthesis of a TMC-95A ketomethylene analogue by cyclization via intramolecular Suzuki coupling. *Org. Lett.* **2003**, *5*, 3435–3437.
- (19) Kaiser, M.; Milbradt, A. G.; Siciliano, C.; Assfalg-Machleidt, I.; Machleidt, W.; Groll, M.; Renner, C.; Moroder, L. TMC-95A analogues with endocyclic biphenyl ether group as proteasome inhibitors. *Chem. Biodiversity* **2004**, *1*, 161–173.
- (20) Groll, M.; Götz, M.; Kaiser, M.; Weyher, E.; Moroder, L. TMC-95-based inhibitor design provides evidence for the catalytic versatility of the proteasome. *Chem. Biol.* **2006**, *13*, 607–614.
- (21) Berthelot, A.; Piguél, S.; Le Dour, G.; Vidal, J. Synthesis of macrocyclic peptide analogues of proteasome inhibitor TMC-95A. *J. Org. Chem.* **2003**, *68*, 9835–9838.
- (22) Bodanszky, M.; Bodanszky, A. *The Practice of Peptide Synthesis*, 2nd ed.; Springer-Verlag: Berlin, 1994.
- (23) Sy, W.-W. Iodination of methoxyamphetamines with iodine and silver sulfate. *Tetrahedron Lett.* **1993**, *34*, 6223–6224.
- (24) Ishiyama, T.; Murata, M.; Miyaura, N. Palladium(0)-catalyzed cross-coupling reaction of alkoxydiboron with haloarenes: a direct procedure for arylboronic esters. *J. Org. Chem.* **1995**, *60*, 7508–7510.
- (25) Suzuki, A.; Brown, H. C. *Organic Syntheses via Boranes. Suzuki Coupling*; Aldrich Chemical Co.: Milwaukee, WI, 2003; p 20.
- (26) (a) Miyaura, N.; Suzuki, A. Palladium-catalyzed cross-coupling reactions of organoboron compounds. *Chem. Rev.* **1995**, *95*, 2457–2483. (b) Lloyd-Williams, P.; Giralt, E. Atropisomerism, biphenyls and the Suzuki coupling: peptide antibiotics. *Chem. Soc. Rev.* **2001**, *30*, 145–157.
- (27) Hassan, J.; Sevignon, M.; Gozzi, C.; Schulz, E.; Lemaire, M. Aryl–aryl bond formation one century after the discovery of the Ullmann reaction. *Chem. Rev.* **2002**, *102*, 1359–1469.
- (28) (a) Wang, W.; Xiong, C.; Yang, J.; Hruby, V. J. Practical, asymmetric synthesis of aromatic-substituted bulky and hydrophobic tryptophan derivatives. *Tetrahedron Lett.* **2001**, *42*, 7717–7719. (b) Wang, W.; Xiong, C.; Zhang, J.; Hruby, V. J. Practical, asymmetric synthesis of aromatic-substituted bulky and hydrophobic tryptophan and phenylalanine derivatives. *Tetrahedron* **2002**, *58*, 3101–3110.
- (29) Kaiser, M.; Milbradt, A.; Moroder, L. Synthesis of TMC-95A analogues. Structure based prediction of cyclisation propensities of linear precursors. *Leit. Pept. Sci.* **2002**, *65*–70.
- (30) (a) Semmelhack, M. F.; Helquist, P. M.; Jones, L. D. Synthesis with zerovalent nickel. Coupling of aryl halides with bis(1,5-cyclooctadiene)nickel(0). *J. Am. Chem. Soc.* **1971**, *93*, 5908–5910. (b) Carbonnelle, A.-C.; Zamora, E. G.; Beugelmans, R.; Roussi, G. The first synthesis of simplified 16- and 17-membered ring macropolypeptides containing the phenyl-indole system of kistamycin and chloro-peptin I, II. *Tetrahedron Lett.* **1998**, *39*, 4471–4472. (c) Beugelmans, R.; Roussi, G.; Zamora, E. G.; Carbonnelle, A.-C. Synthetic studies towards western and eastern macropolypeptide subunits of kistamycin. *Tetrahedron* **1999**, *55*, 5089–5112.

- (31) Momose, I.; Umezawa, Y.; Hirosawa, S.; Iinuma, H.; Ikeda, D. Structure-based design of derivatives of tyropeptin A as the potent and selective inhibitors of mammalian 20S proteasome. *Bioorg. Med. Chem. Lett.* **2005**, *15*, 1867–1871.
- (32) Marastoni, M.; Baldisserotto, A.; Canella, A.; Gavioli, R.; De Risi, C.; Pollini, G. P.; Tomatis, R. Arecoline tripeptide inhibitors of proteasome. *J. Med. Chem.* **2004**, *47*, 1587–1590.
- (33) Basse, N.; Papapostolou, D.; Pagano, M.; Reboud-Ravaux, M.; Bernard, E.; Felten, A.-S.; Vanderesse, R. Development of lipopeptides for inhibiting 20S proteasomes. *Bioorg. Med. Chem. Lett.* **2006**, *16*, 3277–3281.
- (34) Lum, R. T.; Nelson, M. G.; Joly, A.; Horsma, A. G.; Lee, G.; Meyer, S. M.; Wick, M. M.; Schow, S. R. Selective inhibition of the chymotrypsin-like activity of the 20S proteasome by 5-methoxy-1-indanone dipeptide benzamides. *Bioorg. Med. Chem. Lett.* **1998**, *8*, 209–214.
- (35) Glenn, R. J.; Pemberton, A. J.; Royle, H. J.; Spackman, R. W.; Smith, E.; Rivett, A. J.; Sterverding, D. Trypanocidal effect of α' , β' -epoxyketones indicates that trypanosomes are particularly sensitive to inhibitors of proteasome trypsin-like activity. *Int. J. Antimicrob. Agents* **2004**, *24*, 286–289.

JM0701324